



Welcome to E-XFL.COM

Understanding [Embedded - FPGAs \(Field Programmable Gate Array\)](#)

Embedded - FPGAs, or Field Programmable Gate Arrays, are advanced integrated circuits that offer unparalleled flexibility and performance for digital systems. Unlike traditional fixed-function logic devices, FPGAs can be programmed and reprogrammed to execute a wide array of logical operations, enabling customized functionality tailored to specific applications. This reprogrammability allows developers to iterate designs quickly and implement complex functions without the need for custom hardware.

Applications of Embedded - FPGAs

The versatility of Embedded - FPGAs makes them indispensable in numerous fields. In telecommunications.

Details

Product Status	Obsolete
Number of LABs/CLBs	-
Number of Logic Elements/Cells	-
Total RAM Bits	36864
Number of I/O	93
Number of Gates	250000
Voltage - Supply	1.425V ~ 1.575V
Mounting Type	Surface Mount
Operating Temperature	0°C ~ 85°C (TJ)
Package / Case	208-BFQFP
Supplier Device Package	208-PQFP (28x28)
Purchase URL	https://www.e-xfl.com/product-detail/microsemi/afs250-pq208

Example: Calculation for Match Count

To put the Fusion device on standby for one hour using an external crystal of 32.768 KHz:

The period of the crystal oscillator is T_{crystal} :

$$T_{\text{crystal}} = 1 / 32.768 \text{ KHz} = 30.518 \mu\text{s}$$

The period of the counter is T_{counter} :

$$T_{\text{counter}} = 30.518 \mu\text{s} \times 128 = 3.90625 \text{ ms}$$

The Match Count for 1 hour is Δtmatch :

$$\Delta\text{tmatch} / T_{\text{counter}} = (1 \text{ hr} \times 60 \text{ min/hr} \times 60 \text{ sec/min}) / 3.90625 \text{ ms} = 921600 \text{ or } 0xE1000$$

Using a 32.768 KHz crystal, the maximum standby time of the 40-bit counter is 4,294,967,296 seconds, which is 136 years.

Table 2-15 • Memory Map for RTC in ACM Register and Description

ACMADDR	Register Name	Description	Use	Default Value
0x40	COUNTER0	Counter bits 7:0	Used to preload the counter to a specified start point.	0x00
0x41	COUNTER1	Counter bits 15:8		0x00
0x42	COUNTER2	Counter bits 23:16		0x00
0x43	COUNTER3	Counter bits 31:24		0x00
0x44	COUNTER4	Counter bits 39:32		0x00
0x48	MATCHREG0	Match register bits 7:0	The RTC comparison bits	0x00
0x49	MATCHREG1	Match register bits 15:8		0x00
0x4A	MATCHREG2	Match register bits 23:16		0x00
0x4B	MATCHREG3	Match register bits 31:24		0x00
0x4C	MATCHREG4	Match register bits 39:32		0x00
0x50	MATCHBIT0	Individual match bits 7:0	The output of the XNOR gates 0 – Not matched 1 – Matched	0x00
0x51	MATCHBIT1	Individual match bits 15:8		0x00
0x52	MATCHBIT2	Individual match bits 23:16		0x00
0x53	MATCHBIT3	Individual match bits 31:24		0x00
0x54	MATCHBIT4	Individual match bits 29:32		0x00
0x58	CTRL_STAT	Control (write/read) / Status (read only) register bits	Refer to Table 2-16 on page 2-35 for details.	0x00

Table 2-16 • RTC Control/Status Register

Bit	Name	Description	Default Value
7	rtc_rst	RTC Reset 1 – Resets the RTC 0 – Deassert reset on after two ACM_CLK cycle.	
6	cntr_en	Counter Enable 1 – Enables the counter; rtc_rst must be deasserted as well. First counter increments after 64 RTCCLK positive edges. 0 – Disables the crystal prescaler but does not reset the counter value. Counter value can only be updated when the counter is disabled.	0
5	vr_en_mat	Voltage Regulator Enable on Match 1 – Enables RTCMATCH and RTCPSMMATCH to output 1 when the counter value equals the Match Register value. This enables the 1.5 V voltage regulator when RTCPSMMATCH connects to the RTCPSMMATCH signal in VRPSM. 0 – RTCMATCH and RTCPSMMATCH output 0 at all times.	0
4:3	xt_mode[1:0]	Crystal Mode Controls RTCXTLMODE[1:0]. Connects to RTC_MODE signal in XTLOSC. XTL_MODE uses this value when xtal_en is 1. See the "Crystal Oscillator" section on page 2-20 for mode configuration.	00
2	rst_cnt_omat	Reset Counter on Match 1 – Enables the sync clear of the counter when the counter value equals the Match Register value. The counter clears on the rising edge of the clock. If all the Match Registers are set to 0, the clear is disabled. 0 – Counter increments indefinitely	0
1	rstb_cnt	Counter Reset, active Low 0 - Resets the 40-bit counter value	0
0	xtal_en	Crystal Enable Controls RTCXTLSEL. Connects to SELMODE signal in XTLOSC. 0 – XTLOSC enables control by FPGA_EN; xt_mode is not used. Sleep mode requires this bit to equal 0. 1 – Enables XTLOSC, XTL_MODE control by xt_mode Standby mode requires this bit to be set to 1. See the "Crystal Oscillator" section on page 2-20 for further details on SELMODE configuration.	0

Access to the FB is controlled by the BUSY signal. The BUSY output is synchronous to the CLK signal. FB operations are only accepted in cycles where BUSY is logic 0.

Write Operation

Write operations are initiated with the assertion of the WEN signal. Figure 2-35 on page 2-45 illustrates the multiple Write operations.

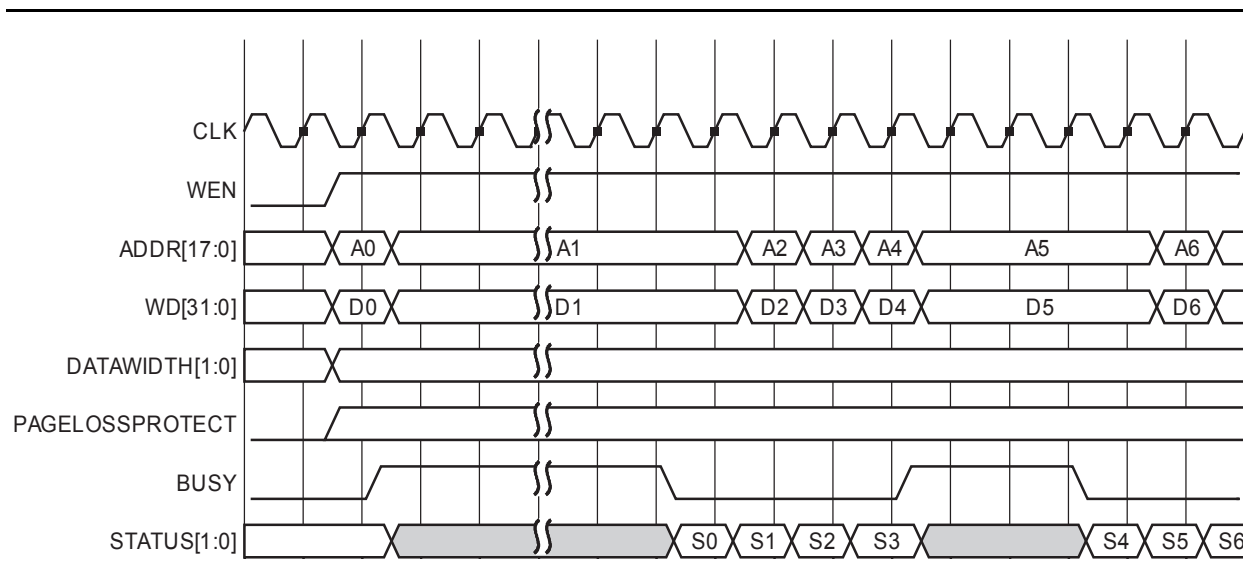


Figure 2-35 • FB Write Waveform

When a Write operation is initiated to a page that is currently not in the Page Buffer, the FB control logic will issue a BUSY signal to the user interface while the page is loaded from the FB Array into the Page Buffer. A Copy Page operation takes no less than 55 cycles and could take more if a Write or Unprotect Page operation is started while the NVM is busy pre-fetching a block. The basic operation is to read a block from the array into the block register (5 cycles) and then write the block register to the page buffer (1 cycle) and if necessary, when the copy is complete, reading the block being written from the page buffer into the block buffer (1 cycle). A page contains 9 blocks, so 9 blocks multiplied by 6 cycles to read/write each block, plus 1 is 55 cycles total. Subsequent writes to the same block of the page will incur no busy cycles. A write to another block in the page will assert BUSY for four cycles (five cycles when PIPE is asserted), to allow the data to be written to the Page Buffer and have the current block loaded into the Block Buffer.

Write operations are considered successful as long as the STATUS output is '00'. A non-zero STATUS indicates that an error was detected during the operation and the write was not performed. Note that the STATUS output is "sticky"; it is unchanged until another operation is started.

Only one word can be written at a time. Write word width is controlled by the DATAWIDTH bus. Users are responsible for keeping track of the contents of the Page Buffer and when to program it to the array. Just like a regular RAM, writing to random addresses is possible. Users can write into the Page Buffer in any order but will incur additional BUSY cycles. It is not necessary to modify the entire Page Buffer before saving it to nonvolatile memory.

Write errors include the following:

1. Attempting to write a page that is Overwrite Protected (STATUS = '01'). The write is not performed.
2. Attempting to write to a page that is not in the Page Buffer when Page Loss Protection is enabled (STATUS = '11'). The write is not performed.

SRAM and FIFO

All Fusion devices have SRAM blocks along the north side of the device. Additionally, AFS600 and AFS1500 devices have an SRAM block on the south side of the device. To meet the needs of high-performance designs, the memory blocks operate strictly in synchronous mode for both read and write operations. The read and write clocks are completely independent, and each may operate at any desired frequency less than or equal to 350 MHz. The following configurations are available:

- 4k×1, 2k×2, 1k×4, 512×9 (dual-port RAM—two read, two write or one read, one write)
- 512×9, 256×18 (two-port RAM—one read and one write)
- Sync write, sync pipelined/nonpipelined read

The Fusion SRAM memory block includes dedicated FIFO control logic to generate internal addresses and external flag logic (FULL, EMPTY, AFULL, AEMPTY).

During RAM operation, addresses are sourced by the user logic, and the FIFO controller is ignored. In FIFO mode, the internal addresses are generated by the FIFO controller and routed to the RAM array by internal MUXes. Refer to [Figure 2-47](#) for more information about the implementation of the embedded FIFO controller.

The Fusion architecture enables the read and write sizes of RAMs to be organized independently, allowing for bus conversion. This is done with the WW (write width) and RW (read width) pins. The different D×W configurations are 256×18, 512×9, 1k×4, 2k×2, and 4k×1. For example, the write size can be set to 256×18 and the read size to 512×9.

Both the write and read widths for the RAM blocks can be specified independently with the WW (write width) and RW (read width) pins. The different D×W configurations are 256×18, 512×9, 1k×4, 2k×2, and 4k×1.

Refer to the allowable RW and WW values supported for each of the RAM macro types in [Table 2-27 on page 2-58](#).

When a width of one, two, or four is selected, the ninth bit is unused. For example, when writing 9-bit values and reading 4-bit values, only the first four bits and the second four bits of each 9-bit value are addressable for read operations. The ninth bit is not accessible.

Typical scaling factors are given in Table 2-57 on page 2-130, and the gain error (which contributes to the minimum and maximum) is in Table 2-49 on page 2-117.

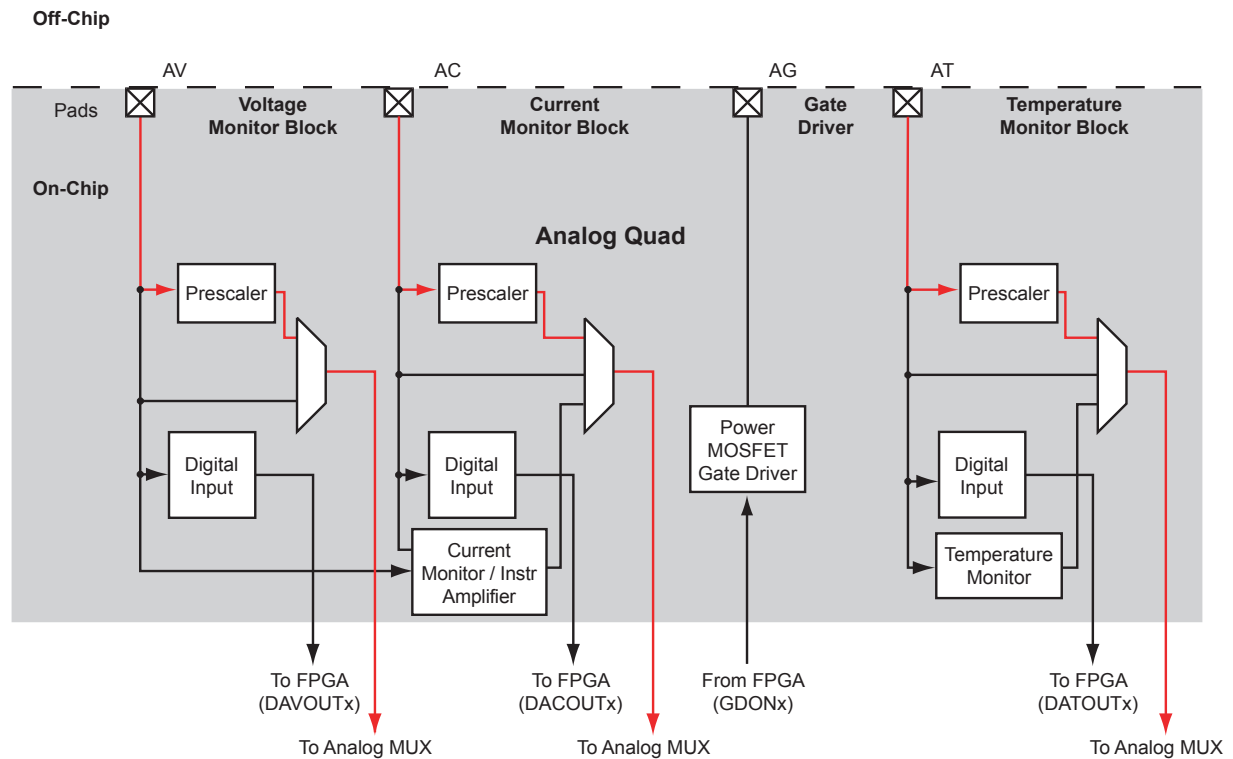


Figure 2-67 • Analog Quad Prescaler Input Configuration

Terminology

BW – Bandwidth

BW is a range of frequencies that a Channel can handle.

Channel

A channel is defined as an analog input configured as one of the Prescaler range shown in Table 2-57 on page 2-130. The channel includes the Prescaler circuit and the ADC.

Channel Gain

Channel Gain is a measure of the deviation of the actual slope from the ideal slope. The slope is measured from the 20% and 80% point.

$$\text{Gain} = \frac{\text{Gain}_{\text{actual}}}{\text{Gain}_{\text{ideal}}}$$

EQ 1

Channel Gain Error

Channel Gain Error is a deviation from the ideal slope of the transfer function. The Prescaler Gain Error is expressed as the percent difference between the actual and ideal, as shown in EQ 2.

$$\text{Error}_{\text{Gain}} = (1 - \text{Gain}) \times 100\%$$

EQ 2

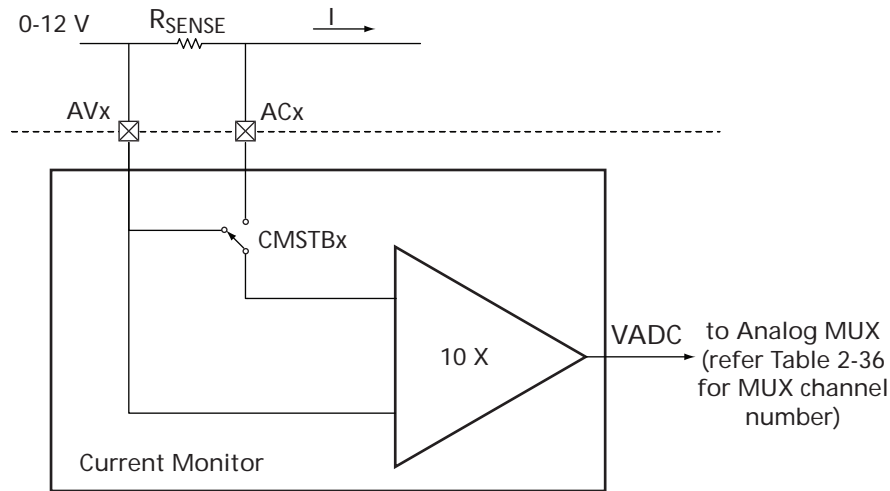


Figure 2-72 • Positive Current Monitor

Care must be taken when choosing the right resistor for current measurement application. Note that because of the 10× amplification, the maximum measurable difference between the AV and AC pads is $V_{AREF} / 10$. A larger AV-to-AC voltage drop will result in ADC saturation; that is, the digital code put out by the ADC will stay fixed at the full scale value. Therefore, the user must select the external sense resistor appropriately. Table 2-38 shows recommended resistor values for different current measurement ranges. When choosing resistor values for a system, there is a trade-off between measurement accuracy and power consumption. Choosing a large resistor will increase the voltage drop and hence increase accuracy of the measurement; however the larger voltage drop dissipates more power ($P = I^2 \times R$).

The Current Monitor is a unipolar system, meaning that the differential voltage swing must be from 0 V to $V_{AREF}/10$. Therefore, the Current Monitor only supports differential voltage where $|V_{AV}-V_{AC}|$ is greater than 0 V. This results in the requirement that the potential of the AV pad must be larger than the potential of the AC pad. This is straightforward for positive voltage systems. For a negative voltage system, it means that the AV pad must be "more negative" than the AC pad. This is shown in Figure 2-73.

In this case, both the AV pad and the AC pad are configured for negative operations and the output of the differential amplifier still falls between 0 V and V_{AREF} as required.

Table 2-37 • Recommended Resistor for Different Current Range Measurement

Current Range	Recommended Minimum Resistor Value (Ohms)
> 5 mA – 10 mA	10 – 20
> 10 mA – 20 mA	5 – 10
> 20 mA – 50 mA	2.5 – 5
> 50 mA – 100 mA	1 – 2
> 100 mA – 200 mA	0.5 – 1
> 200 mA – 500 mA	0.3 – 0.5
> 500 mA – 1 A	0.1 – 0.2
> 1 A – 2 A	0.05 – 0.1
> 2 A – 4 A	0.025 – 0.05
> 4 A – 8 A	0.0125 – 0.025
> 8 A – 12 A	0.00625 – 0.02

This process results in a binary approximation of VIN. Generally, there is a fixed interval T, the sampling period, between the samples. The inverse of the sampling period is often referred to as the sampling frequency $f_s = 1 / T$. The combined effect is illustrated in [Figure 2-82](#).

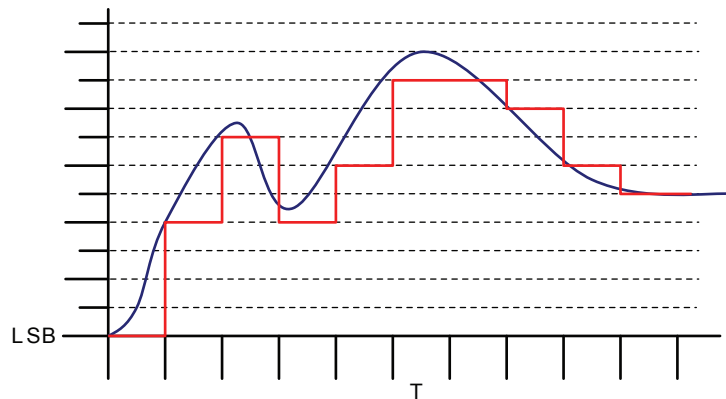


Figure 2-82 • Conversion Example

[Figure 2-82](#) demonstrates that if the signal changes faster than the sampling rate can accommodate, or if the actual value of VIN falls between counts in the result, this information is lost during the conversion. There are several techniques that can be used to address these issues.

First, the sampling rate must be chosen to provide enough samples to adequately represent the input signal. Based on the Nyquist-Shannon Sampling Theorem, the minimum sampling rate must be at least twice the frequency of the highest frequency component in the target signal (Nyquist Frequency). For example, to recreate the frequency content of an audio signal with up to 22 KHz bandwidth, the user must sample it at a minimum of 44 ksps. However, as shown in [Figure 2-82](#), significant post-processing of the data is required to interpolate the value of the waveform during the time between each sample.

Similarly, to re-create the amplitude variation of a signal, the signal must be sampled with adequate resolution. Continuing with the audio example, the dynamic range of the human ear (the ratio of the amplitude of the threshold of hearing to the threshold of pain) is generally accepted to be 135 dB, and the dynamic range of a typical symphony orchestra performance is around 85 dB. Most commercial recording media provide about 96 dB of dynamic range using 16-bit sample resolution. But 16-bit fidelity does not necessarily mean that you need a 16-bit ADC. As long as the input is sampled at or above the Nyquist Frequency, post-processing techniques can be used to interpolate intermediate values and reconstruct the original input signal to within desired tolerances.

If sophisticated digital signal processing (DSP) capabilities are available, the best results are obtained by implementing a reconstruction filter, which is used to interpolate many intermediate values with higher resolution than the original data. Interpolating many intermediate values increases the effective number of samples, and higher resolution increases the effective number of bits in the sample. In many cases, however, it is not cost-effective or necessary to implement such a sophisticated reconstruction algorithm. For applications that do not require extremely fine reproduction of the input signal, alternative methods can enhance digital sampling results with relatively simple post-processing. The details of such techniques are out of the scope of this chapter; refer to the [Improving ADC Results through Oversampling and Post-Processing of Data](#) white paper for more information.

Intra-Conversion

Performing a conversion during power-up calibration is possible but should be avoided, since the performance is not guaranteed, as shown in [Table 2-49 on page 2-117](#). This is described as intra-conversion. [Figure 2-92 on page 2-113](#) shows intra-conversion, (conversion that starts during power-up calibration).

Injected Conversion

A conversion can be interrupted by another conversion. Before the current conversion is finished, a second conversion can be started by issuing a pulse on signal ADCSTART. When a second conversion is issued before the current conversion is completed, the current conversion would be dropped and the ADC would start the second conversion on the rising edge of the SYSCLK. This is known as injected conversion. Since the ADC is synchronous, the minimum time to issue a second conversion is two clock cycles of SYSCLK after the previous one. [Figure 2-93 on page 2-113](#) shows injected conversion, (conversion that starts before a previously started conversion is finished). The total time for calibration still remains 3,840 ADCCLK cycles.

ADC Example

This example shows how to choose the correct settings to achieve the fastest sample time in 10-bit mode for a system that runs at 66 MHz. Assume the acquisition times defined in [Table 2-44 on page 2-108](#) for 10-bit mode, which gives 0.549 μs as a minimum hold time.

The period of SYSCLK: $t_{\text{SYSCLK}} = 1/66 \text{ MHz} = 0.015 \mu\text{s}$

Choosing TVC between 1 and 33 will meet the maximum and minimum period for the ADCCLK requirement. A higher TVC leads to a higher ADCCLK period.

The minimum TVC is chosen so that t_{distrib} and $t_{\text{post-cal}}$ can be run faster. The period of ADCCLK with a TVC of 1 can be computed by [EQ 24](#).

$$t_{\text{ADCCLK}} = 4 \times (1 + \text{TVC}) \times t_{\text{SYSCLK}} = 4 \times (1 + 1) \times 0.015 \mu\text{s} = 0.12 \mu\text{s}$$

EQ 24

The STC value can now be computed by using the minimum sample/hold time from [Table 2-44 on page 2-108](#), as shown in [EQ 25](#).

$$\text{STC} = \frac{t_{\text{sample}}}{t_{\text{ADCCLK}}} - 2 = \frac{0.549 \mu\text{s}}{0.12 \mu\text{s}} - 2 = 4.575 - 2 = 2.575$$

EQ 25

You must round up to 3 to accommodate the minimum sample time requirement. The actual sample time, t_{sample} , with an STC of 3, is now equal to 0.6 μs , as shown in [EQ 26](#)

$$t_{\text{sample}} = (2 + \text{STC}) \times t_{\text{ADCCLK}} = (2 + 3) \times t_{\text{ADCCLK}} = 5 \times 0.12 \mu\text{s} = 0.6 \mu\text{s}$$

EQ 26

Microsemi recommends post-calibration for temperature drift over time, so post-calibration is enabled.

The post-calibration time, $t_{\text{post-cal}}$, can be computed by [EQ 27](#). The post-calibration time is 0.24 μs .

$$t_{\text{post-cal}} = 2 \times t_{\text{ADCCLK}} = 0.24 \mu\text{s}$$

EQ 27

The distribution time, t_{distrib} , is equal to 1.2 μs and can be computed as shown in [EQ 28](#) (N is number of bits, referring back to [EQ 8 on page 2-94](#)).

$$t_{\text{distrib}} = N \times t_{\text{ADCCLK}} = 10 \times 0.12 = 1.2 \mu\text{s}$$

EQ 28

The total conversion time can now be summated, as shown in [EQ 29](#) (referring to [EQ 23 on page 2-109](#)).

$$t_{\text{sync_read}} + t_{\text{sample}} + t_{\text{distrib}} + t_{\text{post-cal}} + t_{\text{sync_write}} = (0.015 + 0.60 + 1.2 + 0.24 + 0.015) \mu\text{s} = 2.07 \mu\text{s}$$

EQ 29

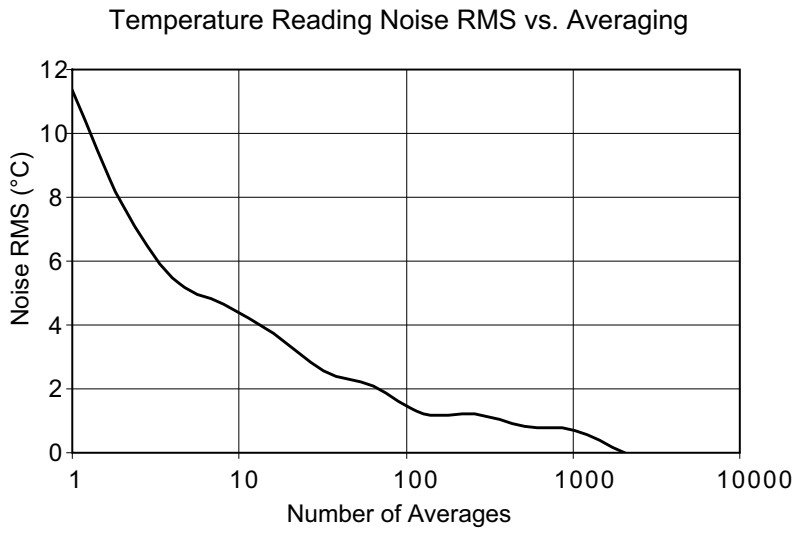


Figure 2-96 • Temperature Reading Noise When Averaging is Used

Analog System Characteristics

Table 2-49 • Analog Channel Specifications
 Commercial Temperature Range Conditions, $T_J = 85^\circ\text{C}$ (unless noted otherwise),
 Typical: $V_{CC33A} = 3.3\text{ V}$, $V_{CC} = 1.5\text{ V}$

Parameter	Description	Condition	Min.	Typ.	Max.	Units
Voltage Monitor Using Analog Pads AV, AC and AT (using prescaler)						
	Input Voltage (Prescaler)	Refer to Table 3-2 on page 3-3				
VINAP	Uncalibrated Gain and Offset Errors	Refer to Table 2-51 on page 2-122				
	Calibrated Gain and Offset Errors	Refer to Table 2-52 on page 2-123				
	Bandwidth ¹				100	KHz
	Input Resistance	Refer to Table 3-3 on page 3-4				
	Scaling Factor	Prescaler modes (Table 2-57 on page 2-130)				
	Sample Time		10			μs
Current Monitor Using Analog Pads AV and AC						
VRSM ¹	Maximum Differential Input Voltage				VAREF / 10	mV
	Resolution	Refer to "Current Monitor" section				
	Common Mode Range				- 10.5 to +12	V
CMRR	Common Mode Rejection Ratio	DC – 1 KHz		60		dB
		1 KHz - 10 KHz		50		dB
		> 10 KHz		30		dB
t_{CMSHI}	Strobe High time		ADC conv. time		200	μs
t_{CMSHI}	Strobe Low time		5			μs
t_{CMSHI}	Settling time		0.02			μs
	Accuracy	Input differential voltage > 50 mV			-2 –(0.05 x VRSM) to +2 + (0.05 x VRSM)	mV

Notes:

1. VRSM is the maximum voltage drop across the current sense resistor.
2. Analog inputs used as digital inputs can tolerate the same voltage limits as the corresponding analog pad. There is no reliability concern on digital inputs as long as VIND does not exceed these limits.
3. VIND is limited to $V_{CC33A} + 0.2$ to allow reaching 10 MHz input frequency.
4. An averaging of 1,024 samples (LPF setting in Analog System Builder) is required and the maximum capacitance allowed across the AT pins is 500 pF.
5. The temperature offset is a fixed positive value.
6. The high current mode has a maximum power limit of 20 mW. Appropriate current limit resistors must be used, based on voltage on the pad.
7. When using SmartGen Analog System Builder, CalibIP is required to obtain specified offset. For further details on CalibIP, refer to the "Temperature, Voltage, and Current Calibration in Fusion FPGAs" chapter of the Fusion FPGA Fabric User Guide.

Summary of I/O Timing Characteristics – Default I/O Software Settings

Table 2-90 • Summary of AC Measuring Points
Applicable to All I/O Bank Types

Standard	Input Reference Voltage (VREF_TYP)	Board Termination Voltage (VTT_REF)	Measuring Trip Point (Vtrip)
3.3 V LVTTTL / 3.3 V LVCMOS	–	–	1.4 V
2.5 V LVCMOS	–	–	1.2 V
1.8 V LVCMOS	–	–	0.90 V
1.5 V LVCMOS	–	–	0.75 V
3.3 V PCI	–	–	0.285 * VCCI (RR) 0.615 * VCCI (FF))
3.3 V PCI-X	–	–	0.285 * VCCI (RR) 0.615 * VCCI (FF)
3.3 V GTL	0.8 V	1.2 V	VREF
2.5 V GTL	0.8 V	1.2 V	VREF
3.3 V GTL+	1.0 V	1.5 V	VREF
2.5 V GTL+	1.0 V	1.5 V	VREF
HSTL (I)	0.75 V	0.75 V	VREF
HSTL (II)	0.75 V	0.75 V	VREF
SSTL2 (I)	1.25 V	1.25 V	VREF
SSTL2 (II)	1.25 V	1.25 V	VREF
SSTL3 (I)	1.5 V	1.485 V	VREF
SSTL3 (II)	1.5 V	1.485 V	VREF
LVDS	–	–	Cross point
LVPECL	–	–	Cross point

Table 2-91 • I/O AC Parameter Definitions

Parameter	Definition
t _{DP}	Data to Pad delay through the Output Buffer
t _{PY}	Pad to Data delay through the Input Buffer with Schmitt trigger disabled
t _{DOUT}	Data to Output Buffer delay through the I/O interface
t _{EOUT}	Enable to Output Buffer Tristate Control delay through the I/O interface
t _{DIN}	Input Buffer to Data delay through the I/O interface
t _{PYS}	Pad to Data delay through the Input Buffer with Schmitt trigger enabled
t _{HZ}	Enable to Pad delay through the Output Buffer—High to Z
t _{ZH}	Enable to Pad delay through the Output Buffer—Z to High
t _{LZ}	Enable to Pad delay through the Output Buffer—Low to Z
t _{ZL}	Enable to Pad delay through the Output Buffer—Z to Low
t _{ZHS}	Enable to Pad delay through the Output Buffer with delayed enable—Z to High
t _{ZLS}	Enable to Pad delay through the Output Buffer with delayed enable—Z to Low

Table 2-115 • 2.5 V LVC MOS High Slew
Commercial Temperature Range Conditions: $T_J = 70^\circ\text{C}$, Worst-Case $V_{CC} = 1.425\text{ V}$,
Worst-Case $V_{CCI} = 2.3\text{ V}$
Applicable to Advanced I/Os

Drive Strength	Speed Grade	t_{DOUT}	t_{DP}	t_{DIN}	t_{PY}	t_{EOUT}	t_{ZL}	t_{ZH}	t_{LZ}	t_{HZ}	t_{ZLS}	t_{ZHS}	Units
4 mA	Std.	0.66	8.66	0.04	1.31	0.43	7.83	8.66	2.68	2.30	10.07	10.90	ns
	-1	0.56	7.37	0.04	1.11	0.36	6.66	7.37	2.28	1.96	8.56	9.27	ns
	-2	0.49	6.47	0.03	0.98	0.32	5.85	6.47	2.00	1.72	7.52	8.14	ns
8 mA	Std.	0.66	5.17	0.04	1.31	0.43	5.04	5.17	3.05	3.00	7.27	7.40	ns
	-1	0.56	4.39	0.04	1.11	0.36	4.28	4.39	2.59	2.55	6.19	6.30	ns
	-2	0.49	3.86	0.03	0.98	0.32	3.76	3.86	2.28	2.24	5.43	5.53	ns
12 mA	Std.	0.66	3.56	0.04	1.31	0.43	3.63	3.43	3.30	3.44	5.86	5.67	ns
	-1	0.56	3.03	0.04	1.11	0.36	3.08	2.92	2.81	2.92	4.99	4.82	ns
	-2	0.49	2.66	0.03	0.98	0.32	2.71	2.56	2.47	2.57	4.38	4.23	ns
16 mA	Std.	0.66	3.35	0.04	1.31	0.43	3.41	3.06	3.36	3.55	5.65	5.30	ns
	-1	0.56	2.85	0.04	1.11	0.36	2.90	2.60	2.86	3.02	4.81	4.51	ns
	-2	0.49	2.50	0.03	0.98	0.32	2.55	2.29	2.51	2.65	4.22	3.96	ns
24 mA	Std.	0.66	3.56	0.04	1.31	0.43	3.63	3.43	3.30	3.44	5.86	5.67	ns
	-1	0.56	3.03	0.04	1.11	0.36	3.08	2.92	2.81	2.92	4.99	4.82	ns
	-2	0.49	2.66	0.03	0.98	0.32	2.71	2.56	2.47	2.57	4.38	4.23	ns

Note: For the derating values at specific junction temperature and voltage supply levels, refer to Table 3-7 on page 3-9.

Table 2-116 • 2.5 V LVC MOS Low Slew
Commercial Temperature Range Conditions: $T_J = 70^\circ\text{C}$, Worst-Case $V_{CC} = 1.425\text{ V}$,
Worst-Case $V_{CCI} = 2.3\text{ V}$
Applicable to Standard I/Os

Drive Strength	Speed Grade	t_{DOUT}	t_{DP}	t_{DIN}	t_{PY}	t_{EOUT}	t_{ZL}	t_{ZH}	t_{LZ}	t_{HZ}	Units
2 mA	Std.	0.66	11.00	0.04	1.29	0.43	10.37	11.00	2.03	1.83	ns
	-1	0.56	9.35	0.04	1.10	0.36	8.83	9.35	1.73	1.56	ns
	-2	0.49	8.21	0.03	0.96	0.32	7.75	8.21	1.52	1.37	ns
4 mA	Std.	0.66	11.00	0.04	1.29	0.43	10.37	11.00	2.03	1.83	ns
	-1	0.56	9.35	0.04	1.10	0.36	8.83	9.35	1.73	1.56	ns
	-2	0.49	8.21	0.03	0.96	0.32	7.75	8.21	1.52	1.37	ns
6 mA	Std.	0.66	7.50	0.04	1.29	0.43	7.36	7.50	2.39	2.46	ns
	-1	0.56	6.38	0.04	1.10	0.36	6.26	6.38	2.03	2.10	ns
	-2	0.49	5.60	0.03	0.96	0.32	5.49	5.60	1.78	1.84	ns
8 mA	Std.	0.66	7.50	0.04	1.29	0.43	7.36	7.50	2.39	2.46	ns
	-1	0.56	6.38	0.04	1.10	0.36	6.26	6.38	2.03	2.10	ns
	-2	0.49	5.60	0.03	0.96	0.32	5.49	5.60	1.78	1.84	ns

Note: For the derating values at specific junction temperature and voltage supply levels, refer to Table 3-7 on page 3-9.

3.3 V PCI, 3.3 V PCI-X

The Peripheral Component Interface for 3.3 V standard specifies support for 33 MHz and 66 MHz PCI Bus applications.

Table 2-134 • Minimum and Maximum DC Input and Output Levels

3.3 V PCI/PCI-X	VIL		VIH		VOL	VOH	IOL	IOH	IOSL	IOSH	IIL ¹	IIH ²
	Min. V	Max. V	Min. V	Max. V	Max. V	Min. V	mA	mA	Max. mA ³	Max. mA ³	μA ⁴	μA ⁴
Per PCI specification	Per PCI curves										10	10

Notes:

1. IIL is the input leakage current per I/O pin over recommended operation conditions where $-0.3\text{ V} < V_{IN} < V_{IL}$.
2. IIH is the input leakage current per I/O pin over recommended operating conditions $V_{IH} < V_{IN} < V_{CCI}$. Input current is larger when operating outside recommended ranges.
3. Currents are measured at high temperature (100°C junction temperature) and maximum voltage.
4. Currents are measured at 85°C junction temperature.

AC loadings are defined per the PCI/PCI-X specifications for the datapath; Microsemi loadings for enable path characterization are described in [Figure 2-123](#).

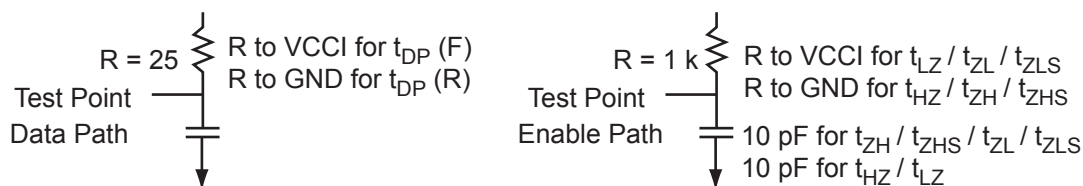


Figure 2-123 • AC Loading

AC loadings are defined per PCI/PCI-X specifications for the data path; Microsemi loading for tristate is described in [Table 2-135](#).

Table 2-135 • AC Waveforms, Measuring Points, and Capacitive Loads

Input Low (V)	Input High (V)	Measuring Point* (V)	VREF (typ.) (V)	C _{LOAD} (pF)
0	3.3	0.285 * VCCI for t _{DP(R)} 0.615 * VCCI for t _{DP(F)}	–	10

Note: *Measuring point = V_{trip}. See [Table 2-90 on page 2-166](#) for a complete table of trip points.

Table 2-169 • AC Waveforms, Measuring Points, and Capacitive Loads

Input Low (V)	Input High (V)	Measuring Point* (V)	VREF (typ.) (V)
1.075	1.325	Cross point	–

Note: *Measuring point = V_{trip} . See Table 2-90 on page 2-166 for a complete table of trip points.

Timing Characteristics

Table 2-170 • LVDS

Commercial Temperature Range Conditions: $T_J = 70^\circ\text{C}$, Worst-Case VCC = 1.425 V,
Worst-Case VCCI = 2.3 V
Applicable to Pro I/Os

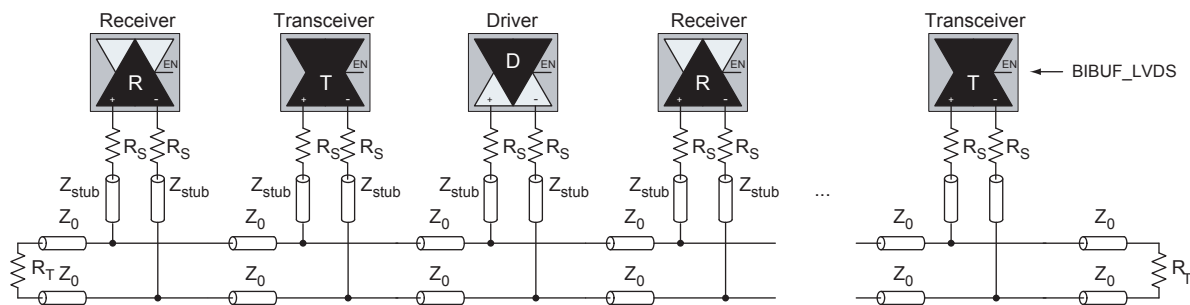
Speed Grade	t_{DOUT}	t_{DP}	t_{DIN}	t_{PY}	Units
Std.	0.66	2.10	0.04	1.82	ns
–1	0.56	1.79	0.04	1.55	ns
–2	0.49	1.57	0.03	1.36	ns

Note: For the derating values at specific junction temperature and voltage supply levels, refer to Table 3-7 on page 3-9.

BLVDS/M-LVDS

Bus LVDS (BLVDS) and Multipoint LVDS (M-LVDS) specifications extend the existing LVDS standard to high-performance multipoint bus applications. Multidrop and multipoint bus configurations can contain any combination of drivers, receivers, and transceivers. Microsemi LVDS drivers provide the higher drive current required by BLVDS and M-LVDS to accommodate the loading. The driver requires series terminations for better signal quality and to control voltage swing. Termination is also required at both ends of the bus, since the driver can be located anywhere on the bus. These configurations can be implemented using TRIBUF_LVDS and BIBUF_LVDS macros along with appropriate terminations. Multipoint designs using Microsemi LVDS macros can achieve up to 200 MHz with a maximum of 20 loads. A sample application is given in Figure 2-135. The input and output buffer delays are available in the LVDS section in Table 2-171.

Example: For a bus consisting of 20 equidistant loads, the following terminations provide the required differential voltage, in worst-case industrial operating conditions at the farthest receiver: $R_S = 60\ \Omega$ and $R_T = 70\ \Omega$, given $Z_0 = 50\ \Omega$ (2") and $Z_{stub} = 50\ \Omega$ (~1.5").


Figure 2-135 • BLVDS/M-LVDS Multipoint Application Using LVDS I/O Buffers

I/O Register Specifications

Fully Registered I/O Buffers with Synchronous Enable and Asynchronous Preset

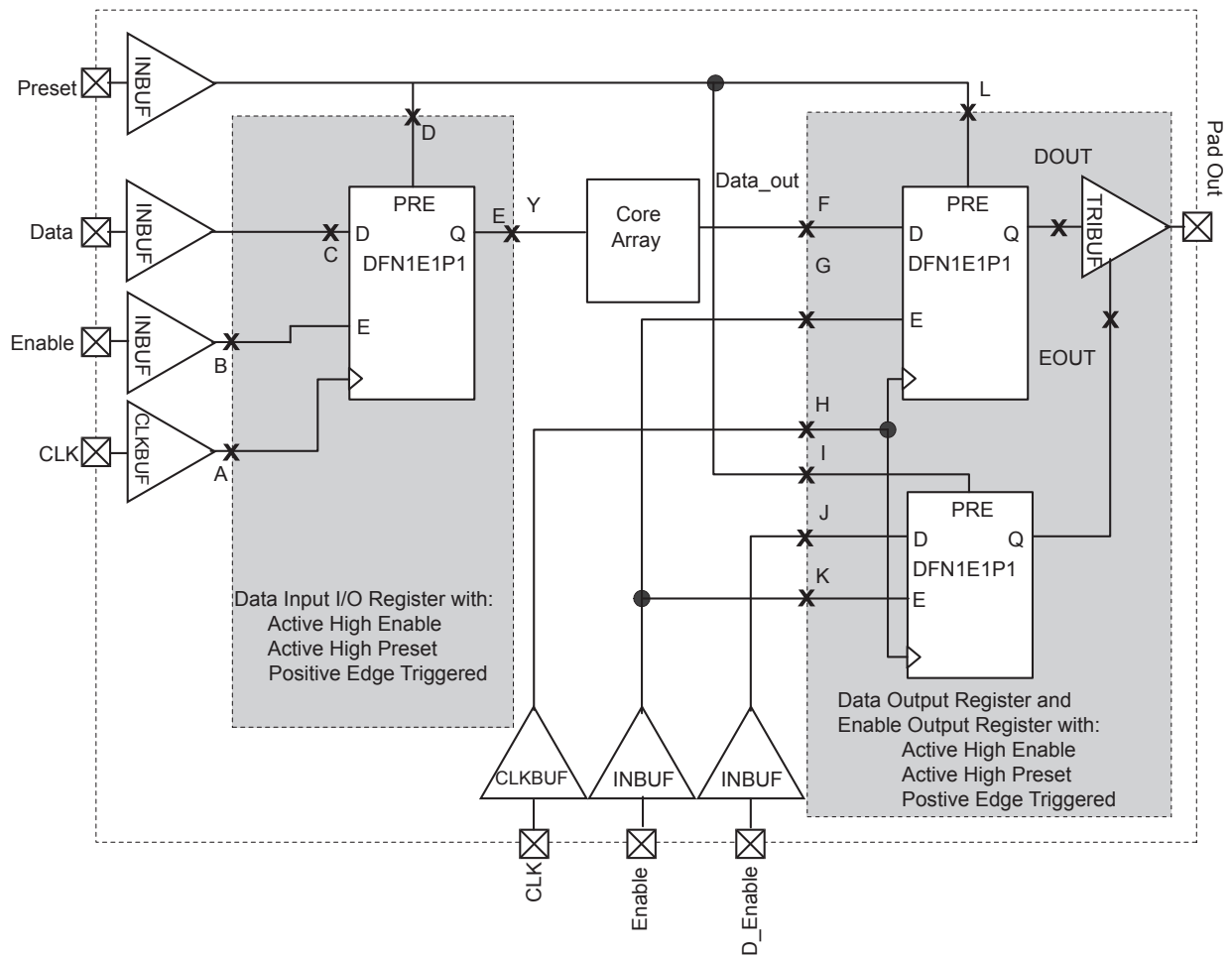


Figure 2-137 • Timing Model of Registered I/O Buffers with Synchronous Enable and Asynchronous Preset

Dynamic Power Consumption of Various Internal Resources

Table 3-14 • Different Components Contributing to the Dynamic Power Consumption in Fusion Devices

Parameter	Definition	Power Supply		Device-Specific Dynamic Contributions				Units
		Name	Setting	AFS1500	AFS600	AFS250	AFS090	
PAC1	Clock contribution of a Global Rib	VCC	1.5 V	14.5	12.8	11	11	μW/MHz
PAC2	Clock contribution of a Global Spine	VCC	1.5 V	2.5	1.9	1.6	0.8	μW/MHz
PAC3	Clock contribution of a VersaTile row	VCC	1.5 V	0.81				μW/MHz
PAC4	Clock contribution of a VersaTile used as a sequential module	VCC	1.5 V	0.11				μW/MHz
PAC5	First contribution of a VersaTile used as a sequential module	VCC	1.5 V	0.07				μW/MHz
PAC6	Second contribution of a VersaTile used as a sequential module	VCC	1.5 V	0.29				μW/MHz
PAC7	Contribution of a VersaTile used as a combinatorial module	VCC	1.5 V	0.29				μW/MHz
PAC8	Average contribution of a routing net	VCC	1.5 V	0.70				μW/MHz
PAC9	Contribution of an I/O input pin (standard dependent)	VCCI	See Table 3-12 on page 3-18					
PAC10	Contribution of an I/O output pin (standard dependent)	VCCI	See Table 3-13 on page 3-20					
PAC11	Average contribution of a RAM block during a read operation	VCC	1.5 V	25				μW/MHz
PAC12	Average contribution of a RAM block during a write operation	VCC	1.5 V	30				μW/MHz
PAC13	Dynamic Contribution for PLL	VCC	1.5 V	2.6				μW/MHz
PAC15	Contribution of NVM block during a read operation (F < 33MHz)	VCC	1.5 V	358				μW/MHz
PAC16	1st contribution of NVM block during a read operation (F > 33 MHz)	VCC	1.5 V	12.88				mW
PAC17	2nd contribution of NVM block during a read operation (F > 33 MHz)	VCC	1.5 V	4.8				μW/MHz
PAC18	Crystal Oscillator contribution	VCC33A	3.3 V	0.63				mW
PAC19	RC Oscillator contribution	VCC33A	3.3 V	3.3				mW
PAC20	Analog Block dynamic power contribution of ADC	VCC	1.5 V	3				mW

Methodology

Total Power Consumption— P_{TOTAL}

Operating Mode, Standby Mode, and Sleep Mode

$$P_{TOTAL} = P_{STAT} + P_{DYN}$$

P_{STAT} is the total static power consumption.

P_{DYN} is the total dynamic power consumption.

Total Static Power Consumption— P_{STAT}

Operating Mode

$$P_{STAT} = PDC1 + (N_{NVM-BLOCKS} * PDC4) + PDC5 + (N_{QUADS} * PDC6) + (N_{INPUTS} * PDC7) + (N_{OUTPUTS} * PDC8) + (N_{PLLS} * PDC9)$$

$N_{NVM-BLOCKS}$ is the number of NVM blocks available in the device.

N_{QUADS} is the number of Analog Quads used in the design.

N_{INPUTS} is the number of I/O input buffers used in the design.

$N_{OUTPUTS}$ is the number of I/O output buffers used in the design.

N_{PLLS} is the number of PLLs available in the device.

Standby Mode

$$P_{STAT} = PDC2$$

Sleep Mode

$$P_{STAT} = PDC3$$

Total Dynamic Power Consumption— P_{DYN}

Operating Mode

$$P_{DYN} = P_{CLOCK} + P_{S-CELL} + P_{C-CELL} + P_{NET} + P_{INPUTS} + P_{OUTPUTS} + P_{MEMORY} + P_{PLL} + P_{NVM} + P_{XTL-OSC} + P_{RC-OSC} + P_{AB}$$

Standby Mode

$$P_{DYN} = P_{XTL-OSC}$$

Sleep Mode

$$P_{DYN} = 0 \text{ W}$$

Global Clock Dynamic Contribution— P_{CLOCK}

Operating Mode

$$P_{CLOCK} = (PAC1 + N_{SPINE} * PAC2 + N_{ROW} * PAC3 + N_{S-CELL} * PAC4) * F_{CLK}$$

N_{SPINE} is the number of global spines used in the user design—guidelines are provided in the "Spine Architecture" section of the Global Resources chapter in the *Fusion and Extended Temperature Fusion FPGA Fabric User's Guide*.

N_{ROW} is the number of VersaTile rows used in the design—guidelines are provided in the "Spine Architecture" section of the Global Resources chapter in the *Fusion and Extended Temperature Fusion FPGA Fabric User's Guide*.

F_{CLK} is the global clock signal frequency.

N_{S-CELL} is the number of VersaTiles used as sequential modules in the design.

Standby Mode and Sleep Mode

$$P_{CLOCK} = 0 \text{ W}$$

Sequential Cells Dynamic Contribution— P_{S-CELL}

Operating Mode

PQ208		
Pin Number	AFS250 Function	AFS600 Function
147	GCC1/IO47PDB1V0	IO39NDB2V0
148	IO42NDB1V0	GCA2/IO39PDB2V0
149	GBC2/IO42PDB1V0	IO31NDB2V0
150	VCCIB1	GBB2/IO31PDB2V0
151	GND	IO30NDB2V0
152	VCC	GBA2/IO30PDB2V0
153	IO41NDB1V0	VCCIB2
154	GBB2/IO41PDB1V0	GNDQ
155	IO40NDB1V0	VCOMPLB
156	GBA2/IO40PDB1V0	VCCPLB
157	GBA1/IO39RSB0V0	VCCIB1
158	GBA0/IO38RSB0V0	GNDQ
159	GBB1/IO37RSB0V0	GBB1/IO27PPB1V1
160	GBB0/IO36RSB0V0	GBA1/IO28PPB1V1
161	GBC1/IO35RSB0V0	GBB0/IO27NPB1V1
162	VCCIB0	GBA0/IO28NPB1V1
163	GND	VCCIB1
164	VCC	GND
165	GBC0/IO34RSB0V0	VCC
166	IO33RSB0V0	GBC1/IO26PDB1V1
167	IO32RSB0V0	GBC0/IO26NDB1V1
168	IO31RSB0V0	IO24PPB1V1
169	IO30RSB0V0	IO23PPB1V1
170	IO29RSB0V0	IO24NPB1V1
171	IO28RSB0V0	IO23NPB1V1
172	IO27RSB0V0	IO22PPB1V0
173	IO26RSB0V0	IO21PPB1V0
174	IO25RSB0V0	IO22NPB1V0
175	VCCIB0	IO21NPB1V0
176	GND	IO20PSB1V0
177	VCC	IO19PSB1V0
178	IO24RSB0V0	IO14NSB0V1
179	IO23RSB0V0	IO12PDB0V1
180	IO22RSB0V0	IO12NDB0V1
181	IO21RSB0V0	VCCIB0
182	IO20RSB0V0	GND
183	IO19RSB0V0	VCC

PQ208		
Pin Number	AFS250 Function	AFS600 Function
184	IO18RSB0V0	IO10PPB0V1
185	IO17RSB0V0	IO09PPB0V1
186	IO16RSB0V0	IO10NPB0V1
187	IO15RSB0V0	IO09NPB0V1
188	VCCIB0	IO08PPB0V1
189	GND	IO07PPB0V1
190	VCC	IO08NPB0V1
191	IO14RSB0V0	IO07NPB0V1
192	IO13RSB0V0	IO06PPB0V0
193	IO12RSB0V0	IO05PPB0V0
194	IO11RSB0V0	IO06NPB0V0
195	IO10RSB0V0	IO04PPB0V0
196	IO09RSB0V0	IO05NPB0V0
197	IO08RSB0V0	IO04NPB0V0
198	IO07RSB0V0	GAC1/IO03PDB0V0
199	IO06RSB0V0	GAC0/IO03NDB0V0
200	GAC1/IO05RSB0V0	VCCIB0
201	VCCIB0	GND
202	GND	VCC
203	VCC	GAB1/IO02PDB0V0
204	GAC0/IO04RSB0V0	GAB0/IO02NDB0V0
205	GAB1/IO03RSB0V0	GAA1/IO01PDB0V0
206	GAB0/IO02RSB0V0	GAA0/IO01NDB0V0
207	GAA1/IO01RSB0V0	GNDQ
208	GAA0/IO00RSB0V0	VCCIB0

Revision	Changes	Page
Revision 2 (continued)	A note was added to Figure 2-27 • Real-Time Counter System (not all the signals are shown for the AB macro) stating that the user is only required to instantiate the VRPSM macro if the user wishes to specify PUPO behavior of the voltage regulator to be different from the default, or employ user logic to shut the voltage regulator off (SAR 21773).	2-31
	VPUMP was incorrectly represented as VPP in several places. This was corrected to VPUMP in the "Standby and Sleep Mode Circuit Implementation" section and Table 3-8 • AFS1500 Quiescent Supply Current Characteristics through Table 3-11 • AFS090 Quiescent Supply Current Characteristics (21963).	2-32, 3-10
	Additional information was added to the Flash Memory Block "Write Operation" section, including an explanation of the fact that a copy-page operation takes no less than 55 cycles (SAR 26338).	2-45
	The "FlashROM" section was revised to refer to Figure 2-46 • FlashROM Timing Diagram and Table 2-26 • FlashROM Access Time rather than stating 20 MHz as the maximum FlashROM access clock and 10 ns as the time interval for D0 to become valid or invalid (SAR 22105).	2-53, 2-54
	The following figures were deleted (SAR 29991). Reference was made to a new application note, <i>Simultaneous Read-Write Operations in Dual-Port SRAM for Flash-Based cSoCs and FPGAs</i> , which covers these cases in detail (SAR 34862). Figure 2-55 • Write Access after Write onto Same Address Figure 2-56 • Read Access after Write onto Same Address Figure 2-57 • Write Access after Read onto Same Address	2-63, 2-66, 2-65, 2-75
	The port names in the SRAM "Timing Waveforms", "Timing Characteristics", SRAM tables, Figure 2-55 • RAM Reset. Applicable to both RAM4K9 and RAM512x18. , and the FIFO "Timing Characteristics" tables were revised to ensure consistency with the software names (SAR 35753).	
	In several places throughout the datasheet, GNDREF was corrected to ADCGNDREF (SAR 20783): Figure 2-64 • Analog Block Macro Table 2-36 • Analog Block Pin Description "ADC Operation" section	2-77 2-78 2-104
	The following note was added below Figure 2-78 • Timing Diagram for the Temperature Monitor Strobe Signal : When the IEEE 1149.1 Boundary Scan EXTEST instruction is executed, the AG pad drive strength ceases and becomes a 1 μ A sink into the Fusion device. (SAR 24796).	2-93
	The "Analog-to-Digital Converter Block" section was extensively revised, reorganizing the information and adding the "ADC Theory of Operation" section and "Acquisition Time or Sample Time Control" section. The "ADC Example" section was reworked and corrected (SAR 20577).	2-96
	Table 2-49 • Analog Channel Specifications was modified to include calibrated and uncalibrated values for offset (AFS090 and AFS250) for the external and internal temperature monitors. The "Offset" section was revised accordingly and now references Table 2-49 • Analog Channel Specifications (SARs 22647, 27015).	2-95, 2-117
The "Intra-Conversion" section and "Injected Conversion" section had definitions incorrectly interchanged and have been corrected. Figure 2-92 • Intra-Conversion Timing Diagram and Figure 2-93 • Injected Conversion Timing Diagram were also incorrectly interchanged and have been replaced correctly. Reference in the figure notes to EQ 10 has been corrected to EQ 23 (SAR 20547).	2-110, 2-113, 2-113	

Revision	Changes	Page
Advance v0.8 (continued)	The voltage range in the "VPUMP Programming Supply Voltage" section was updated. The parenthetical reference to "pulled up" was removed from the statement, "VPUMP can be left floating or can be tied (pulled up) to any voltage between 0 V and 3.6 V."	2-225
	The "ATRTNx Temperature Monitor Return" section was updated with information about grounding and floating the pin.	2-226
	The following text was deleted from the "VREF I/O Voltage Reference" section: (all digital I/O).	2-225
	The "NCAP Negative Capacitor" section and "PCAP Positive Capacitor" section were updated to include information about the type of capacitor that is required to connect the two.	2-228
	1 μ F was changed to 100 pF in the "XTAL1 Crystal Oscillator Circuit Input".	2-228
	The "Programming" section was updated to include information about V_{CCOSC} .	2-229
	The VMV pins have now been tied internally with the V_{CCI} pins.	N/A
	The AFS090 "108-Pin QFN" table was updated.	3-2
	The AFS090 and AFS250 devices were updated in the "108-Pin QFN" table.	3-2
	The AFS250 device was updated in the "208-Pin PQFP" table.	3-8
	The AFS600 device was updated in the "208-Pin PQFP" table.	3-8
	The AFS090, AFS250, AFS600, and AFS1500 devices were updated in the "256-Pin FBGA" table.	3-12
	The AFS600 and AFS1500 devices were updated in the "484-Pin FBGA" table.	3-20
Advance v0.7 (January 2007)	The AFS600 device was updated in the "676-Pin FBGA" table.	3-28
	The AFS1500 digital I/O count was updated in the "Fusion Family" table.	I
	The AFS1500 digital I/O count was updated in the "Package I/Os: Single-/Double-Ended (Analog)" table.	II
Advance v0.6 (October 2006)	The second paragraph of the "PLL Macro" section was updated to include information about POWERDOWN.	2-30
	The description for bit 0 was updated in Table 2-17 · RTC Control/Status Register.	2-38
	3.9 was changed to 7.8 in the "Crystal Oscillator (Xtal Osc)" section.	2-40.
	All function descriptions in Table 2-18 · Signals for VRPSM Macro.	2-42
	In Table 2-19 · Flash Memory Block Pin Names, the RD[31:0] description was updated.	2-43
	The "RESET" section was updated.	2-61
	The "RESET" section was updated.	2-64
	Table 2-35 · FIFO was updated.	2-79
	The VAREF function description was updated in Table 2-36 · Analog Block Pin Description.	2-82
	The "Voltage Monitor" section was updated to include information about low power mode and sleep mode.	2-86
	The text in the "Current Monitor" section was changed from 2 mV to 1 mV.	2-90
The "Gate Driver" section was updated to include information about forcing 1 V on the drain.	2-94	